VOL. 12, NO. 11, JUNE 2017 ISSN 1819-6608
ARPN Journal of Engineering and Applied Sciences

www.arpnjournals.com

SHOCK WAVES IN A CHANNEL WITH A CENTRAL BODY

A. N. Ryabinin
Department of Hydroaeromechanics, Faculty of Mathematics and Mechanics, Saint-Petersburg State University, St. Petersburg, Russia
E-Mail: a.ryabinin@spbu.ru

ABSTRACT

Positions of shock waves in the 2D channel with a central body are studied numerically. Solutions of the Euler equations and Reynolds-averaged Navier–Stokes equations are obtained with finite-volume solvers. Numerical simulations reveal a considerable hysteresis in the shock wave position versus the supersonic Mach number given at the inlet for inviscid gas and for viscous gas. In the certain range of inlet Mach number, there are asymmetrical solutions of the equations. Small change in the geometry of the channel leads to shift of the hysteresis range.

Keywords: shock wave position, computational fluid dynamics, hysteresis.

INTRODUCTION

It was shown that the transonic flow near the airfoil with surface of small curvature is sensitive to the small change in the free stream velocity and in the angle of attack [1-5]. Sensitivity is caused by the interaction of local supersonic regions near the airfoil. Two supersonic regions exist near the surface of small curvature. The leading supersonic region is terminated by shock wave. Behind the shock, the flow is subsonic. Behind subsonic line, the flow is supersonic again. Increasing in the Mach number leads to arising of two supersonic regions. The distance between regions decreases. However, it could not be zero. At the moment of coalescence of two regions the shock position abruptly changes. Further decreasing of inflow Mach number leads to splitting of supersonic region. However, splitting occurs at inflow Mach number that is less than Mach number of coalescence. Computations reveal a hysteresis in the shock position versus the inflow Mach number. A review of studies on this topic is published in [5].

Problems of the shock waves instability were studied in [6 - 9] for the channels with wall break or bend. The phenomenon of coalescence and splitting of supersonic regions exists in the channels.

FORMULATION OF THE PROBLEM. A NUMERICAL METHOD

We consider 2D flow in the channel with the central body. Straight segments constitute lower and upper walls of the channel. The channel is diverging. There are central bodies in the channel. The sketches of the channel are presented below in the Figure-1.

Upper and lower walls include breaking points at x= 2.0. Before breaking points:

if $0 \le x \le 2.0$ then $y = \pm 0.88 \pm 0.0521x$.

After breaking points:

if $2.0 \le x \le 3.0$ then $y = \pm 0.9843 \pm 0.229(x - 2.0)$.

Central body consists of three straight segments:

if $1.4 < x \le 3.0$ then $y = \pm 0.01 \pm 0.119(x - 1.4)$,

if $x = 1.4$ then $-0.01 < y < 0.01$.

The coordinates (x, y) are dimensional. Here and further coordinates are given in meters. Inlet and outlet boundaries are vertical straight segments. The angles of expansion of the channel walls coincide with the angles of expansion of the channel studied in [10], but the breaking points are shifted upstream. Two channels with slightly changed geometry are also considered. One of them (variant a) has the central body with enlarged angle of expansion:

if $1.4 < x \le 3.0$ then $y = \pm 0.01 \pm 0.131(x - 1.4)$,
if $x = 1.4$ then $-0.01 < y < 0.01$.

Another channel (variant b) has modified geometry of the walls:

if $0 \le x \le 2.0$ then $y = \pm 0.88 \pm 0.045x$,
if $2.0 \le x \le 3.0$ then $y = \pm 0.97 \pm 0.2429(x - 2.0)$.

Thus, in the range $1.4 \le x \le 2$ parts of all the channels were converging. The converging angle $\beta \approx 3.83$ deg for main variant, $\beta \approx 4.52$ deg for variant a, $\beta \approx 4.24$ deg for variant b.

2D unstructured (for inviscid fluid) or hybrids (for viscous fluid) mesh were generated using package Gmsh [11]. These meshes were used for calculations in the package Stanford University Unstructured (SU^2) [12]. A program written in Pascal language transformed them into 3D meshes, whose lateral size was equal to one element. The transformed meshes are in the TGrid/Fluent format, which is suitable for the calculation in the commercial package Ansys CFX [13]. In the solution of RANS equations, the mesh was fined near the walls. The non-dimensional thickness of the first mesh layer y^+ is less than 1. The vanishing flux of heat is used on the wall. The slip condition for Euler equations and no-slip condition for RANS equations are accepted. Specific heat of air at constant pressure is equal 1004.4 J / (kg K). Molar mass is equal to 28.96 kg/kmol.

The mesh for solution of Euler equations has 110598 elements for main variant of the channel, 110304 elements for variant a, 108990 elements for variant b. The solutions of Reynolds averaged Navier-Stokes (RANS) equations are obtained with the mesh with 149907 elements. At the inflow boundary temperature $T_{in} = 250$ K, inlet Mach number M_{in}, pressure p_{in} or Reynolds number Re for RANS equations on the base of the length of 1 m are set. Solutions of Euler equations are obtained with both SU^2 and Ansys CFX finite volume solvers. Solutions of RANS equations are obtained with Ansys CFX. Reynolds number Re is equal to $5.6 \cdot 10^6$. The model of turbulence k-ω SST is used. Inflow turbulence intensity is equal to 5%.

RESULTS OF CALCULATIONS

At low inletMach number, there is shock wave upstream the central body. Figure-1shows two patterns of Euler equations solutions. Solutions are obtained with SU^2 solver. White line corresponds M = 1. The distance from inlet boundary to shock wave is denoted by x_s as it is shown in the picture.The first pattern a) has two supersonic regions divided by the subsonic one. Inlet Mach number M_{in} is equal 1.281. Small increasing of inlet Mach number up to 1.282 leads to coalescence of supersonic regions. In the second pattern b) supersonic regions coalesce and form the single supersonic region.

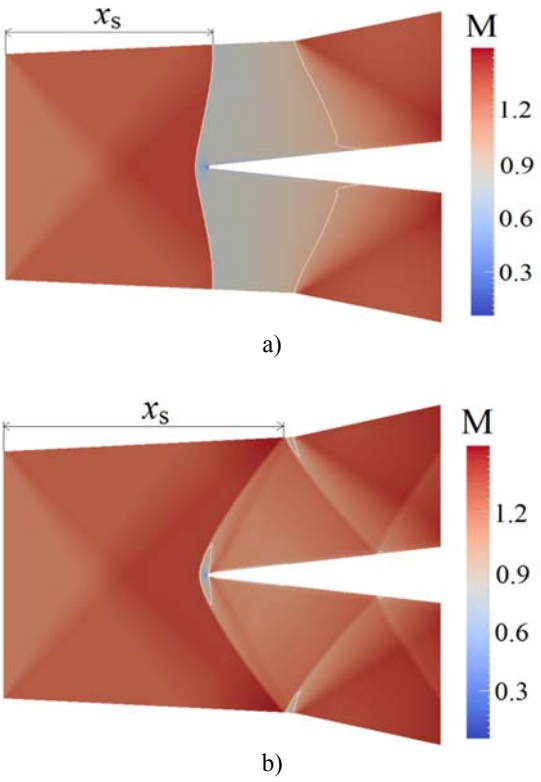

Figure-1. Two patterns of shock wave configuration in the first channel for solutions of Euler equations. Mach number distribution: a) $M_{in} = 1.181$, two supersonic regions, b) $M_{in} = 1.182$, single supersonic region.

Near the walls the oblique shocks are formed. Shock position x_s abruptly changes. There are small subsonic regions upstream the nose of central body and near the walls of the channel. Further reducing of the inlet Mach number leads to a restructuring of shock waves and splitting of supersonic regions at another inlet Mach number. At reduced Mach number the small subsonic regions increases at the walls of the channel and the central body.

Figure-2 shows two patterns. The first pattern a) corresponds $M_{in} = 1.1$. Subsonic regions exist near the walls of the channel and central body. There is the single supersonic region. Another pattern b) demonstrate the merging of small subsonic regions at $M_{in} = 1.08$. Two supersonic regions are separated by narrow subsonic region. However, dramatically change in shock position does not exist.

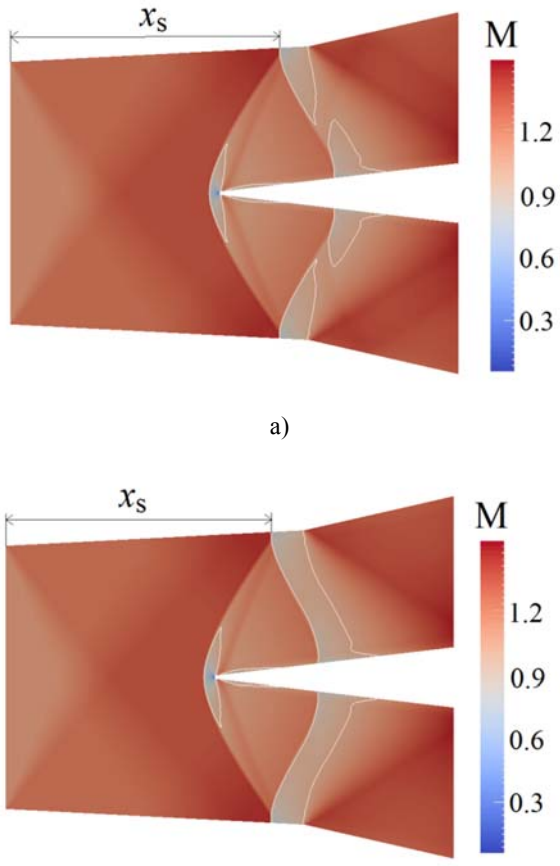

Figure-2. Two patterns of shock wave configuration in the first channel for solutions of Euler equations. Machnumber distribution: a) $M_{in} = 1.1$, single supersonic region, b) $M_{in} = 1.08$, supersonic regions separated by narrow subsonic one.

The further reducing of inlet Mach number corresponds to abruptly change of shock position x_s at $M_{in} = 1.069$. Flow pattern becomes similar to pattern a) in Figure-1.

Asymmetrical solutions of equations can be obtained by introducing of asymmetry in the first stage of calculations. For example in the first stage, angle of attack differs from zero. At the second stage, angle of attack is equal to zero and asymmetrical solution obtained in the first stage is taken as an initial condition. Another way of introducing the asymmetry is different inlet Mach number for upper and lower parts of inlet boundary.

Two asymmetrical flow patterns are presented in the Figure-3. There are two supersonic regions in the upper part of the channel. Regions are separated by a wide subsonic region. The lower part of the channel in the pattern a) includes the single supersonic region. There are two local subsonic regions attached to the walls of the channel and central body.Pattern b) demonstrates the coalescence of the local subsonic regions. So supersonic regions are separated by narrow subsonic region. For asymmetrical solution the distances $x_s$in the upper and lower parts of the channel differ from one another.

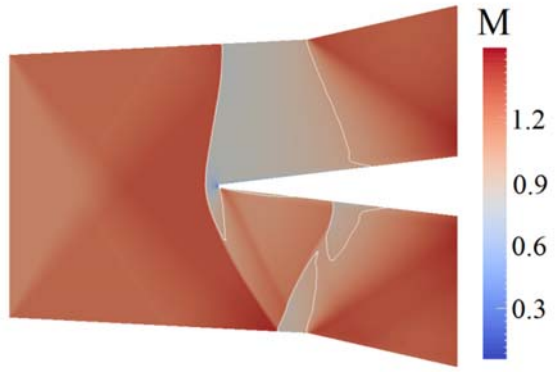

a)

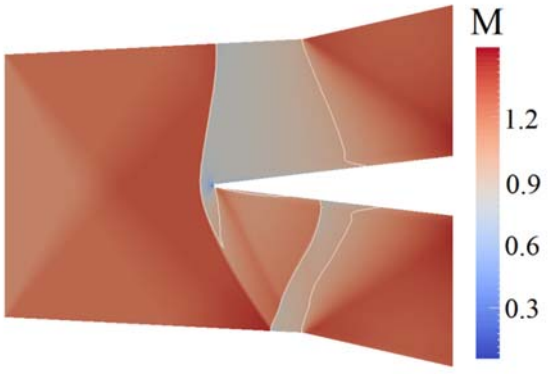

b)

Figure-3. Two asymmetrical flow patterns: a) $M_{in} = 1.14$, b) $M_{in} = 1.135$.

Figure-4 demonstrates hysteresis obtained by two solvers. Both solvers show existence of hysteresis, but ranges of hysteresis differ from one another.

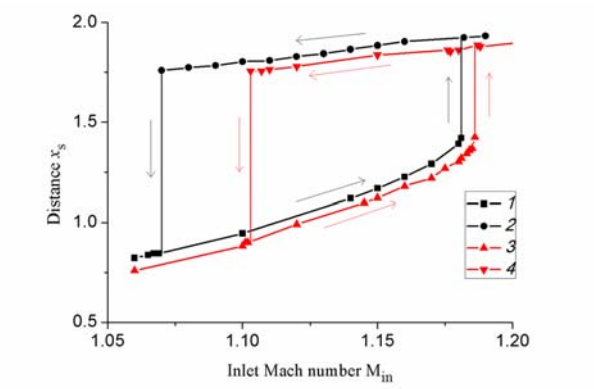

Figure-4. Dependence of distance $x_s$on inlet Mach number for the main channel: *1, 2* - Euler equations SU^2 solver, *3, 4* - RANS equations, Ansys CFX solver. *1*, *3* - pattern with two supersonic regions, *2*, *4*- pattern with single supersonic region or two supersonic regions divided by narrow subsonic region.

The left boundary of the hysteresis range of inlet Mach number for viscous gas is greater than left boundary for inviscid gas. It can be explained by existence of the boundary layer. Growth of the boundary layer leads to the narrowing of cross-section area of the channel. Calculations reveal that for channels variants a and b the hysteresis ranges shift too. This phenomenon is shown in the Figure-5.

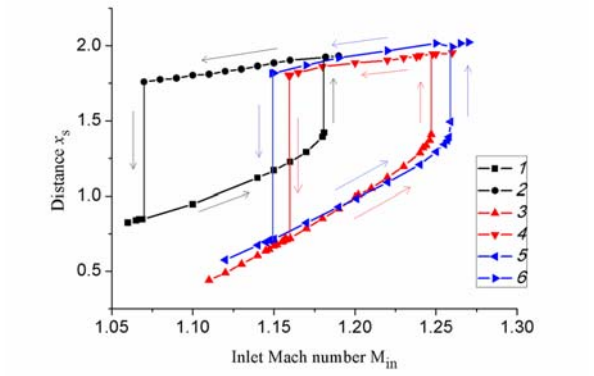

Figure-5. Dependence of distance $x_s$on inflow Mach number for three variants channel, Euler equations: *1, 2* - main channel, SU^2 solver, *3, 4* - variant a, SU^2 solver, *5, 6* -variant b, Ansys CFX solver. *1*, *3, 5* - pattern with two supersonic regions, *2*, *4, 6* - pattern with single supersonic region or two supersonic regions divided by narrow subsonic region.

Hysteresis range is greater than the range of existence of asymmetrical patterns. Figure-6 shows dependence of the distance x_s on the inlet Mach number for symmetrical and asymmetrical patterns for solutions of Euler equations. The similar dependencies can be presented for solutions of RANS equations for main channel and for solutions of Euler equations for channels variants a and b.

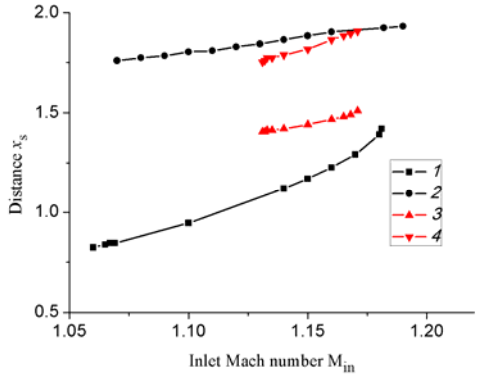

Figure-6. Four regimes of transonic flow in the main channel: *1*- two supersonic region, *2* - single supersonic regions or two supersonic regions divided by narrow subsonic region, *3, 4* - asymmetrical patterns.

Figure-7 demonstrates the dependence of the distance x_s on the inlet Mach number M_{in} for two channels. The shift of the wall breaking point downstream leads to shift of hysteresis diagram to the large inlet Mach number.

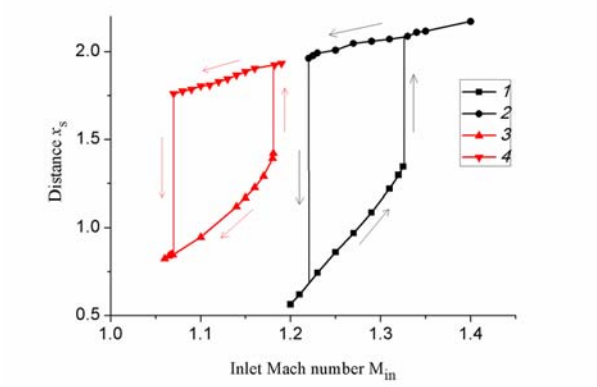

Figure-7. Hysteresis diagrams for main channel (*3, 4*) and for channel studied in [10] (*1, 2*).

CONCLUSIONS

The numerical simulations of 2D transonic flow in the channelwith central body reveal a hysteresis in the shock wave position as the functions of the inlet Mach numbers. The phenomenon exist for inviscid gas and for viscous gas at Re = $5.6 \cdot 10^6$. The left boundary of hysteresis range of inlet Mach number for the viscous gas is greater than the left boundary of the range for the inviscid gas. Small decreasing of converging parts of the channels between channel walls and the central body leads to shift of the boundaries of hysteresis range to greater inlet Mach number. The shift of the wall breaking point downstream leads to shift of hysteresis diagram to the large inlet Mach number. The hysteresis range of inlet Mach number includes the range of existence of asymmetrical solutions of the Euler and Reynolds averaged Navier-Stokes equations.

ACKNOWLEDGEMENT

Studies were performed using computing resources providing by "Computing Center of St. Petersburg State University" (http://cc.spbu.ru).

REFERENCES

[1] Jameson A. Airfoils admitting non-unique solutions of the Euler equations. 1991. AIAA paper no. 91-1625.

[2] Ivanova A.V, Kuzmin A.G. 2004. Nonuniqueness of the transonic flow past an airfoil. Fluid Dynamics. 39: 642-648.

[3] Kuzmin A. 2005. Instability and bifurcation of transonic flow over airfoils. AIAA paper no: 2005-4800.

[4] Kuzmin A. 2009. Bifurcations and buffet of transonic flow past flattened surfaces. Computers & Fluids. 38: 1369-1374.

[5] Kuzmin A. 2012. Non-unique transonic flows over airfoils. Computers & Fluids. 63: 1-8.

[6] Kuzmin A. 2015. Shock wave instability in a channel with an expansion corner. International J. Applied Mechanics. 7(2): 1-9.

[7] Kuzmin A. 2016. Shock wave bifurcation in convergent-divergent channels of rectangular cross section. Shock Waves. 26:741-747.

[8] Kuzmin A. 2016. Shock wave bifurcation in channels with a bend. Arch Appl. Mech. 86:787-795.

[9] Kuzmin A. 2015. Instability of the shock wave/ sonic line interaction. Paris. France. E-print: Centre national de la recherchescientifique. HAL archives, no. 01136894, https://hal.archives-ouvertes.fr/hal-01136894.

[10] Riabinin A., Suleymanov A. 2016. Bifurcation of transonic flow in the channel with a central body. Conference Topical Problems of Fluid Mechanics 2016. Proceedings. pp. 185-190.

[11] Geuzaine Ch., Remacle, J.-F. 2014. Gmsh Reference Manual. University of Liège. Liège. Belgium. 2014. E-print. http://geuz. org/gmsh/doc/texinfo/gmsh.pdf.

[12] Palacios F., Colonno M. R., Aranake A.C., Campos A., Copeland S.R., Economon T.D., Alonso J.J. 2013. Stanford University Unstructured (SU2): An open-

source integrated computational environment for multi-physics simulation and design. 51st AIAA Aerospace Sciences Meeting including the New Horizons Forum and Aerospace Exposition. AIAA paper no. 2013-0287. http://su2.stanford.edu/ documents/SU2_AIAA_ ASM2013.pdf.

[13] ANSYS CFX-Solver Modeling Guide. Release 13.0. 2010. Canonsburg: ANSYS, Inc. p. 604.